

Subsurface and lithological evidences from aeromagnetic data in some parts of the Sokoto Basin, North West Nigeria

A. Adamu¹, O.K. Likkason², A.S. Maigari³, S. Ali² and O. Ologe¹

¹Department of Applied Geophysics, Federal University Birnin Kebbi, Nigeria

²Department of Physics, Abubakar Tafawa Balewa University Bauchi, Nigeria

³Department of Applied Geology, Abubakar Tafawa Balewa University Bauchi, Nigeria

Email: toyin.ologe@gmail.com;

ABSTRACT

In this work, a reconnaissance study is presented to delineate the subsurface and lithological interpretation of the aeromagnetic data. To achieve this goal, several enhancement techniques and filtering processes were carried out on these maps. At first, the total intensity aeromagnetic map is processed through the application of reduction to the magnetic equator technique. Six aeromagnetic data sheets covering some parts of the Sokoto Basin were used. These maps were digitized on a TMI grid. An analysis of the total magnetic field over the area of study was carried out using the aeromagnetic data sets. The following deduction were made: the interpreted lineaments follow a predominantly EW- and NSW-trending orientation, while other orientations in the survey area include NW-, ENE- and, more rarely E-trending structures, the existence of several high short wavelength magnetic closures with steep gradients near the geologic boundary is a strong indication that the basin may not be as large as shown by the geologic map. The residual magnetic field values were employed to obtain the two-dimensional Fourier transforms from which the radial spectrum was extracted. The slopes of the graph of spectral energy against frequency of nine sections were obtained and used to estimate the depth values. The results suggested that the deeper depth of the study area ranges from 1.99 km – 2.83 km while the shallow depth ranges from 0.78 km – 1.25 km in conformity to the delineation of favourable lithological units between cretaceous meta-sediments and Eocene boundary. Finally, the study reveals that structural interpretation based on aeromagnetic data is an efficient tool for frontier exploration for hydrocarbon accumulation and/or other mineralization.

Keywords: Subsurface; Lithological Inferences; Aeromagnetic Data; Sokoto Basin and Spectral Depth Analysis

Received: 24.11.20 **Accepted:** 31.05.21

1. INTRODUCTION

The application of Gravity and Magnetic methods are extensively used for geological interpretations which play an important role in delineating structural features including faults, folds, shear zones, intrusions, porphyries and other areas favorable for hydrocarbon accumulation / or related mineralization (Hinze *et al.*, 2013). These structures are significant in the exploration and localization of mineralized zones. Various authors propose different techniques for the delineation of lithological contacts and geological structures by applying gradient methods (Lala *et al.*, 2011; Verduco *et al.*, 2004; Donovan *et al.*, 1979; McIntyre, 1980; Liu *et al.*, 1996; Langel, 1992; Reid,

1980; Leech *et al.*, 2003; Luyendyk., 1997; Lasky *et al.*, 1997; Minty *et al.*, 2003). Other authors propose using normalized standard deviations (NSTD) based on ratios of the windowed standard deviation of derivatives of the magnetic field (Reid, 1980; Thompson, 1982). The objective of magnetic interpretation was to recognize the geological characteristics of the subsurface lithologies and structures from the anomaly maps. In addition, magnetic prospecting is useful towards description of the intra-sedimentary and supra-basement magnetic sources, such as the shallow dykes and intrusive, that disrupt the normal continuity of the overlying sedimentary sequence (Hesham and Oweis, 2016; Miller and Singh, 1994). This research work is therefore use

modern techniques and more appropriate software to determine the depth to magnetic source within the study area using spectral depth analysis and source parameter imaging (SPI) as a digital filtering tool. This project survey sets out to take advantage by exploring the use of aeromagnetic data as reconnaissance in investigating structural trends in some parts of the Sokoto Basin, Northwestern Nigeria.

2. MATERIAS AND METHODOLOGY

2.1 Physiography and geology of the study area

The study area is geographically located in the semi-arid with a zone of savannah-type vegetation as part of the sub-Saharan Sudan belt of West Africa with an elevation ranging from 160 m - 300 m above sea level (Fig. 1).

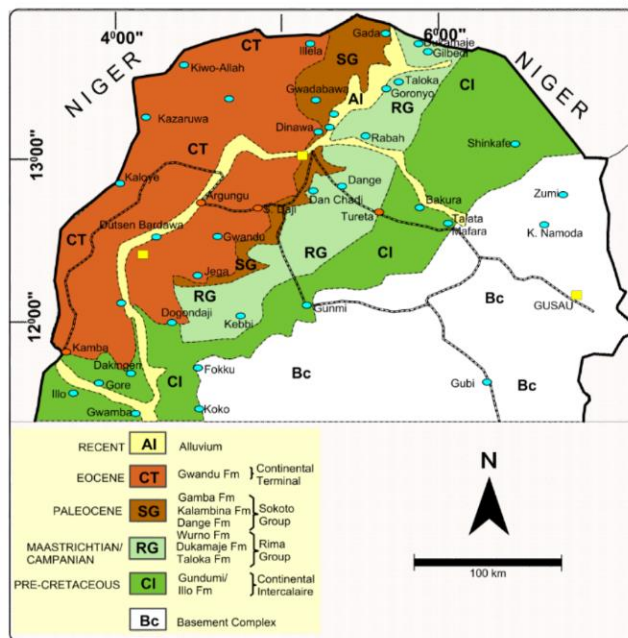


Figure 1: Generalized geological map of the Sokoto Basin (Modified after Kogbe,1978)

The Area enjoys a tropical continental type of climate. Rainfall is concentrated in a short-wet

season, which extends from April to October (Kogbe, 1978; 1979). Mean annual rainfall is about 800 mm-1000 mm while the mean annual temperature ranges from 26.5 to 40°C (Kogbe, 1978). Night temperatures are generally lower. The highest temperature occurs between April and July, the lowest in August (during the rainy season). Relative humidity is generally low (40%) for most of the year except during the wet season when it reaches an average of (80%). This explains the dry environment which is in sharp contrast to a hot humid environment in the southern parts of Nigeria.

The study area is predominantly a gentle undulating plain with an average elevation varying from 250 m - 400 m above sea-level. This plain is occasionally interrupted by low mesas, consists of a number of prominent ridges and groups of flat-topped, steep-sided hills capped by ironstones. The sediments dip gently and thicken gradually towards the northwest with maximum thicknesses attainable towards the border with Niger Republic (Kogbe 1979, 1981, Obaje, 2009).

2.2 Data acquisition and Preparation

The trial was conducted over Birnin Kebbi (Sheet - 49), Tambuwal (Sheet - 50), Giru (Sheet - 72), Dange (Sheet - 29), Sokoto (Sheet – 10) and Fokku (Sheet - 73) of Aeromagnetic Data obtained from Nigerian Geological Survey Agency (NGSA) (Fig. 1). Aeromagnetic surveys had recently been conducted over Nigeria between 2003 and 2009. These were done by Fugro Airborne Surveys on behalf of the Federal Government of Nigeria and the raw grid data in form of total-field magnetic intensity (TMI) are under the custody of the Nigerian Geological Survey Agency (NGSA). Over the Sokoto Basin, the data were collected under the auspices of the World Bank, through the Sustainable Management of Mineral Resources Project (SMMRP) Nigeria commissioning the Fugro Airborne Surveys (Fugro) to conduct the Phase II airborne survey (2007 – 2010), representing the remaining 55% coverage of Nigeria's

landmass. The TMI data have only gone through on-board processing such as magnetic compensation, checking/editing, diurnal correction, tie leveling and micro leveling.

To remove the temporal variation and regional effects, diurnal corrections and the International Geomagnetic Reference Field were applied to the total magnetic intensity data respectively. Prior to applying different filters, the total magnetic intensity (Fig. 4) data were reduced to the equator (RTE) to locate the magnetic anomalies above their source bodies (Fig. 5). Structural complexity analysis of this dataset was achieved through applying the Centre for Exploration Targeting Grid Analysis to the RTE.

Magnetic method of prospecting depends on the potential field characteristics of the subsurface rocks. The method therefore seeks the anomalies arising from changes in the physical properties of the subsurface rocks. Rocks differ in their magnetic mineral content; hence the magnetic anomaly map allows a visualization of the geological structure of the upper crust in the subsurface particularly the spatial geometry of bodies of rock and the presence of faults and folds.

To obtain the spectral depths, the residual field values were divided in to nine square blocks (see Fig. 4). The natural logarithms of the spectral energies together with the wavenumber associated with each square block were estimated. The filed data obtained were later exported into the Microsoft excel work sheets one after the other until the total number of nine spectral energy files were exported. The Microsoft excel worksheet file obtained was later used as an input files into a slope plot program (^{1st}) developed with Matlab. The total numbers of nine spectral energies versus the wave number were plotted with the developed program.

2.3. Analysis of TMI data over the study area

Magnetics is a geophysical survey technique that exploits the considerable differences in the magnetic properties of minerals with the ultimate objective of characterizing the Earth's

subsurface. The technique requires the acquisition of measurements of amplitude of the magnetic field at discrete points along survey lines distributed regularly throughout the survey area. The magnetic is usually measured with a total-field magnetometer. The most common instrument in use today is the cesium vapour magnetometer and proton precession magnetometer. Observations are made at regular intervals along a series of traverse lines of constant azimuth and spacing. Data may be acquired close to the ground level (ground magnetics) via a person carrying a magnetometer. For airborne magnetics (aeromagnetics), data can be acquired via mounting the magnetometer on a fixed wing aircraft or a helicopter which may be necessary where the terrain is rugged. The crustal magnetic field of the Earth which is the field of interest in many ways is often obtained by subtracting from the observed field, the main field and the external field. This crustal field is the magnetic anomaly. The International Geomagnetic Reference Field (IGRF) is considered to be the best available representation of the main field for any particular epoch (Langel 1992; Luyendyk 1997, Mintey *et al.* 2003) and is now almost universally accepted as the background against which magnetic anomalies are reported (Leech *et al.* 2003). The external magnetic field of external sources is often corrected through robust method along with the regular diurnal variation of the order of 20 – 30 nT fully accounted for. It's worth noting that the Earth's magnetic field is largely (>90%) of internal (main field) origin supposedly generated by a dipolar magnetic source located at the Centre of the Earth and nearly aligned with the Earth's rotational axis. The strength of the main field at the magnetic poles is about 60, 000 nT (6×10^5) and nearly half this value at the magnetic equator. The main field is the inducing or polarizing field to all the magnetically susceptible earth materials.

2.4 Analysis of spatial Aliasing effects on survey

Generally, any geophysical anomaly is always larger than the feature causing it. It is therefore

reasonable to choose a station interval that is sufficiently small as to take moreover to be practicable. A point at which a discrete geophysical measurement is made is called a station and the distance between successive measurements is the station intervals. It is fundamental to the success of a survey that the correct choice of station intervals be made. It is a waste of resources to record too many data and equally wasteful if too few are collected. What then is the optimum choice of station interval? This requires some idea of the nature and size of the geological target. Spatial aliasing is the loss of high-frequency information in acquired geophysical data. Spatial aliasing may also occur when gridded data are contoured, particularly by computer software if the grid network is too coarse, high-frequency information may be smeared artificially and appears as lower frequency anomalies. Spatial stretching occurs in datasets acquired along survey lines separated too widely with respect to along-the-line sampling. Similar aliasing problems associated with contouring can arise from radial survey lines and/or too few data points (Reid, 1980). In aeromagnetic surveys, like the one under investigation, the specifications are often agreed contractually before an investigation begins. Even so there are guidelines as to what constitutes an adequate line separation or flight height, orientation of survey line and so on. Reid (1980) has compiled a set of criteria based on avoidance of spatial aliasing. For example, if a mean flying height over magnetic basement (h) of 500 m is used with a flight line spacing (Δx) of 2 km, then the ratio, $h/\Delta x = 0.5/2 = 0.25$, which will indicate that 21% aliasing would occur in measurements of the total field as much as 79% if the vertical magnetic gradient were being measured (see Table 1). Generally, the larger the value of $h/\Delta x \geq 0.5$ depending on the survey type (Reid, 1980), i.e., about 5% maximum aliasing is acceptable if contouring is to be undertaken in total field data.

Table 1: Degree of Aliasing (After Reid 1980).

$h / \Delta x$	F_T (%) aliasing)	F_G (%) aliasing)
0.15	21	56
0.5	4.3	39
1	0.19	5
3	0.0003	0.03
6	0	0

Where F_T and F_G are the aliasing power traction (%) expected from surveys of total field and vertical gradient respectively, h = mean height of sensor above magnetic sources and Δx = sampling or flight line spacing.

3. RESULTS AND DISCUSSION

3.1 Qualitative interpretation of Total Magnetic Intensity (TMI)

The composite total-field aeromagnetic data for the study area are displayed in image (Fig. 2). Images are the most common style or form of presentation today compared to the traditional contour maps. Images are essentially a presentation in which individual pixels in the image (or grey level) are coded according to some attribute of the gridded data being imaged. The advantage of images is that they are capable of showing extremely subtle features not apparent in other forms of presentation (such as contour maps). They can also be quickly manipulated in digital form, thereby providing an ideal basis for on-screen GIS-based applications. Figure 2 is the colour-coded display of display of the TMI data over the study area. The Basement fabrics covering

nearly NWE extending linearly to the southern part (Fig. 2) are characterized by irregular and low-data values compared to the other of the NE side of map which records the peak value. The minimum and maximum values of the gridded data are respectively 32967.3 nT and 33118.7 nT with a standard deviation of 36 having a mean of 33058.6 nT. The area of study is clearly a low magnetic latitude area. The high magnetic intensity values, which dominate the southern part of the study area, perhaps reflect presence of near-surface igneous rocks of high values of magnetic susceptibilities. The low amplitudes are most likely due to sedimentary rocks and other nonmagnetic sources. The scattered highs are areas where the basement is depressed. In general, high magnetic values arise from igneous and crystalline basement rocks, and low magnetic values are usually from sedimentary rocks or altered basement rocks.

3.2 Qualitative interpretation of regional map

Figure 3, shows the regional map of the study area. The trend of the regional map is along ESE-WNW direction ranging from 32835 nT to 32868 nT. The magnetic lows are concentrated in the NE-W part of the study area which shows Higher values appear around the north indicating that the basin is deeper around that area. The southern part in the other hand shows low magnetic anomalies due to near surface basement rocks. This generally agrees with the works of Obaje (2009) and Kamba et al., (2017).

3.3 Qualitative interpretation of residual magnetic map

Figure 4 shows the residual magnetic map of the study area. The residual magnetic value ranges from -55.6 nT to 33.3 nT. Negative magnetic values are more predominant in the east, central and predominant portions in the NW - SE part of the area. This is in agreement with previous results in the study area (Obaje, 2009; Kamba et al., 2017).

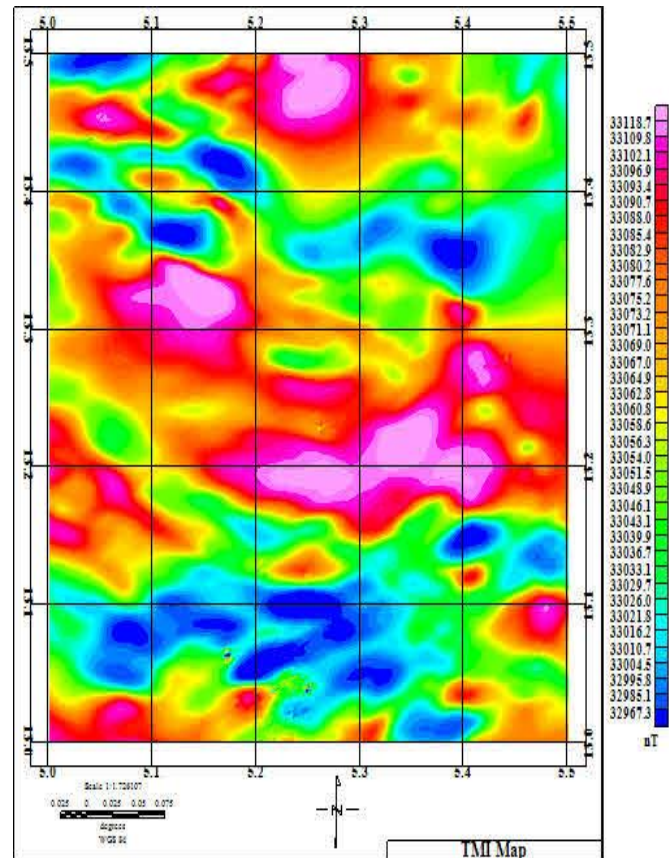


Figure. 2: Total magnetic field intensity (TMI) map of the study area

There are high magnetic values covering the predominant portions of the N-E, extreme lower portion of the S-E of the study area. However, top of the ENW, extreme eastern part and some portions of the extreme S-E of the study area are characterized by low magnetic intensity values. Series of magnetic closures were observed at the central and some portions in the NW and SE of the area. These areas of low magnetic values usually reflect sedimentary rocks or altered basement rocks. This generally agrees with the finding of Liu et al., (1996).

These maps are influences of deeper features as the field is continued upward. Results obtained in figure 5 (a-f) showed that at 2 km and 5 km, with contour values ranging from 55.6 nT to 33.3 nT. The linear features on the maps are still prominent, with blue color

closures dominating NW and EW parts and red-pink colour dominating the SE part.

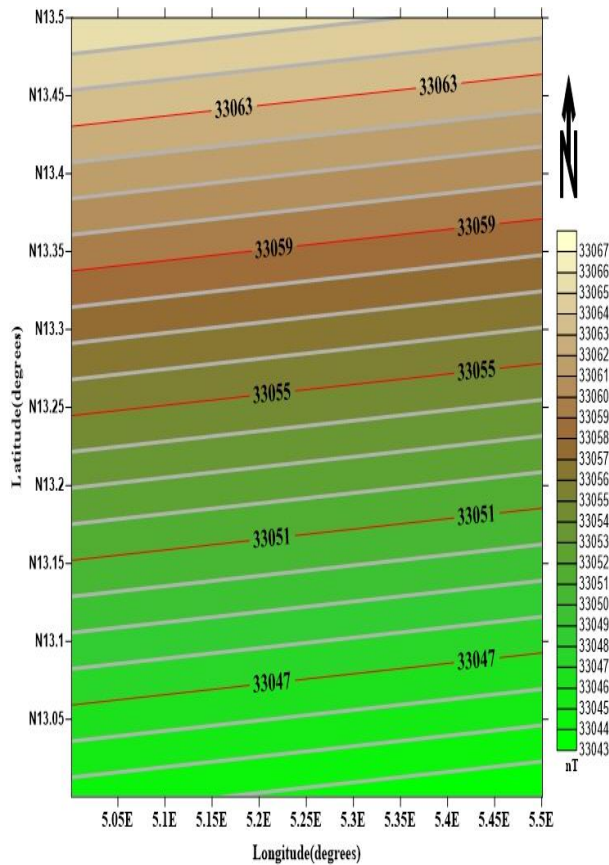


Figure 3: Regional map of the study area

The linear features on the maps are still prominent, with blue color closures dominating NW and EW parts and red-pink colour dominating the SE part.

At 10 km, all the blue colour closures were eliminated except at the northern and eastern part. This clearly shows that the prominence gradually fades out as the height of continuation increases. The SE part still shows red-pink closures, but some portions of anomalies with green colour still exist at the NW part.

At 15 km, the anomalies with green and pink colors at the NW and SE parts were further reduced. This anomaly suggests the presence of a deep-seated lineament (fault) (Kogbe, 1979) within the basement complex of the study area. These lineaments could be a possible target of prolific zones for Hydrocarbon accumulation or mineralization.

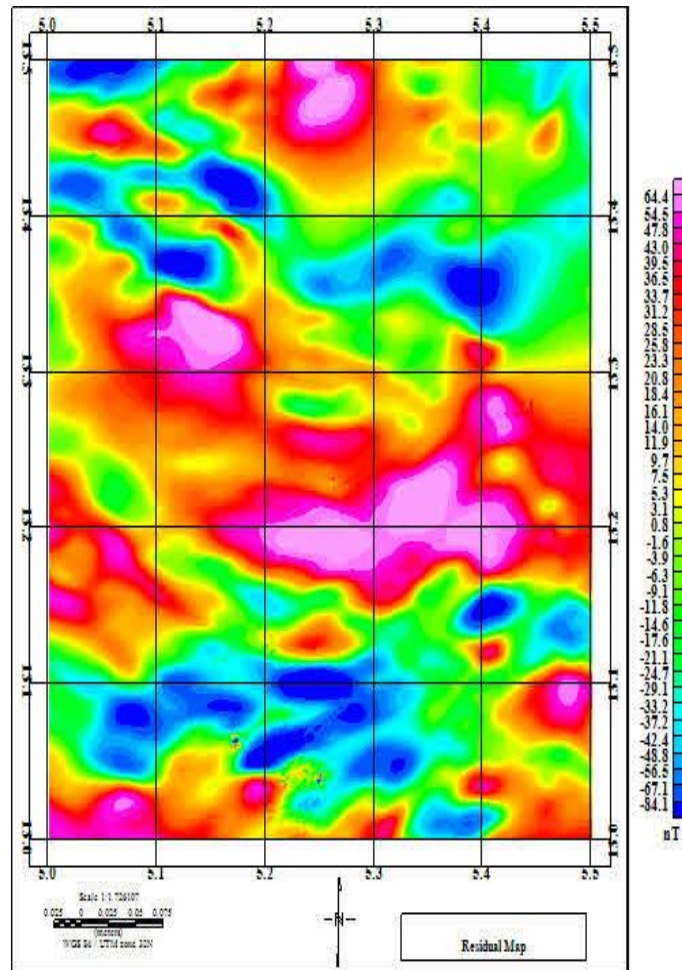


Figure 4: Residual map of the study area

At 20 km, all the anomalies were eliminated except at the SE part. But in the NW part the blue color still persists. The deep-seated lineaments observed at 10 km and 15 km however disappeared, suggesting that they do not extend beyond 15 km.

At 25 km, all the anomalies were eliminated. However, the NW part shows blue color and the SE part is largely dominated by red-pink color. The result of upward continuation at 25 km showed some resemblance with the trend of regional field (E-W).

3.4 Upward continuation

In upward continuation, long wavelength magnetic anomalies emanating from deeper sources are enhanced at the expense of short

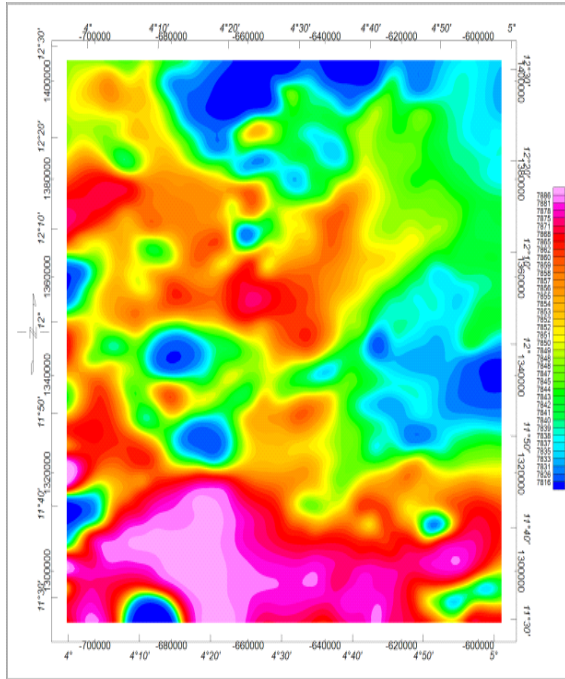
wavelength anomalies emanating from shallow sources. In other words, when residual field is continued upward to different heights above the flight elevation, the short wavelength anomalies are progressively filtered. Thus, the effect of near-surface features being eliminated and enhancing the deeper ones.

Figure 5 (a-f) in Appendix 'A' shows the regional map obtained by continuing the residual field map, upward to 2 km, 5 km, 10 km, 15 km, 20 km, and 25

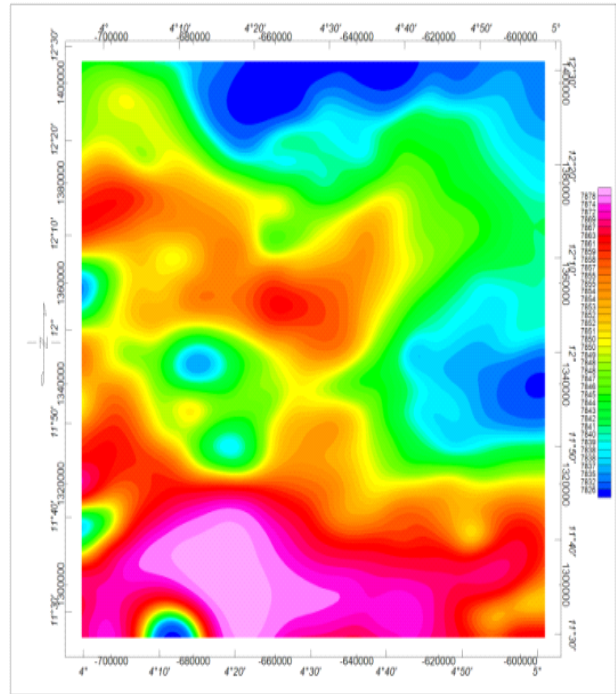
At 20 km, all the anomalies were eliminated except at the SE part. But in the NW part the blue color still persists. The deep-seated lineaments observed at 10 km and 15 km however disappeared, suggesting that they do not extend beyond 15 km.

However, the NW part shows blue color and the

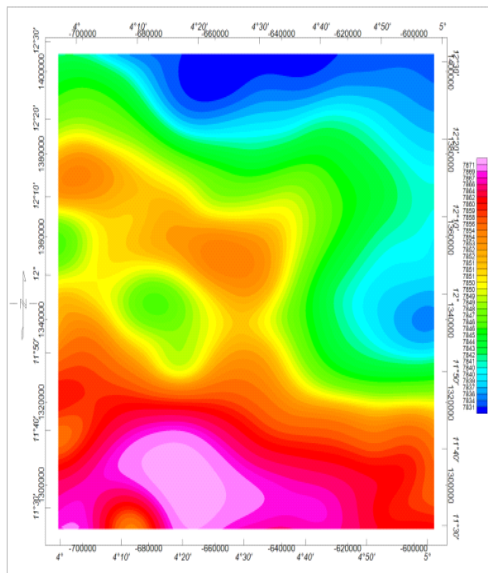
SE part is largely dominated by red-pink color. The result of upward continuation at 25 km showed some resemblance with the trend of regional field (E-W).



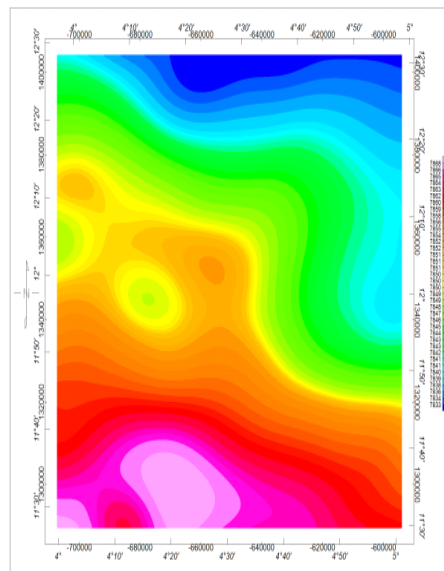
Height of continuum = 2 km
(a)



Height of continuation = 5 km
(b)

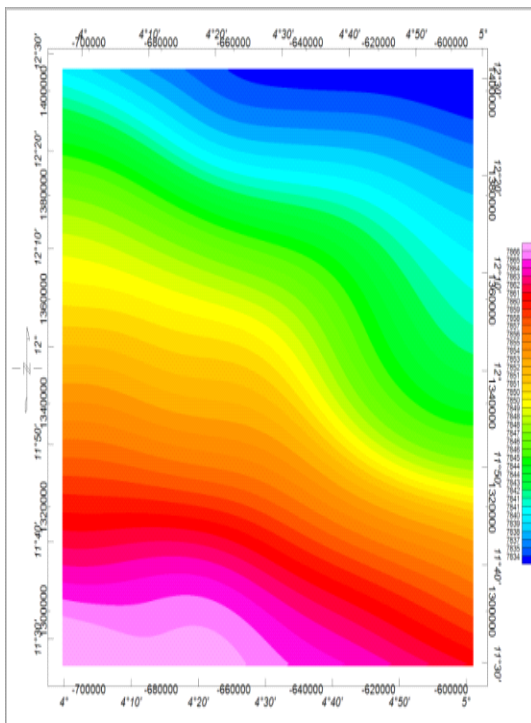


Height of continuation = 10 km
(c)



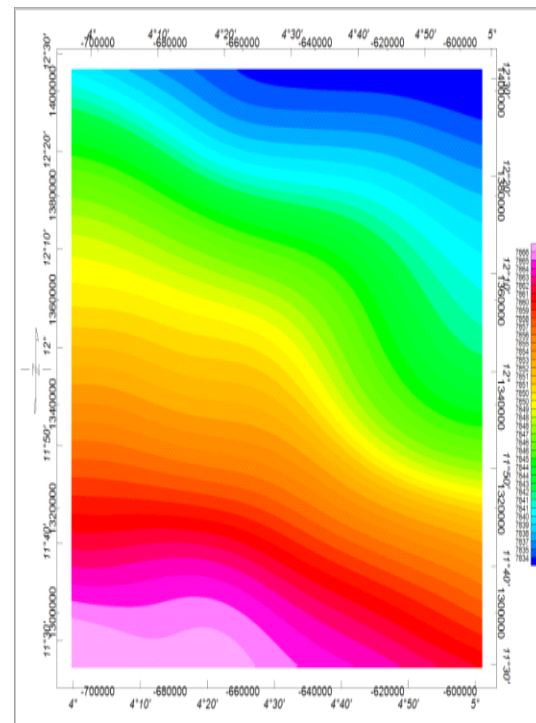
Height of continuation = 15 km
(d)

Figure 5(a-d): Upward continuation fields at various heights



(e)

Height of continuation = 20 km



(f)

Height of continuation = 25 km

Figure 5(e-f): Upward continuation fields at various Heights

3.5 Spectral depth estimation

A typical energy spectrum for magnetic data may exhibit two parts. The low wave number component, which reflects deeper sources, and the high wave number component which reflects shallow sources. The plots of energy against frequency (wave number) are shown in Figures 6 (a-d). From the slopes of the plot, the first- and second-layer magnetic source depths were respectively estimated using linear regression analysis. Two linear segments could be seen from the graphs. The first points on the frequency scale were ignored because the low frequency components in the energy spectrum are generated from the deepest layers. Each linear segment or groups of points are attributed to anomalies within a particular depth. If z is the mean depth of the layer, the

depth factor for this ensemble of anomalies is $\exp(-2zk)$, Thus the logarithmic plot of the radial spectrum against the wave number (k) would give a straight line whose slope is $-2z$.

Table 2, shows the estimated depth of magnetic sources for both the shallow depth (H_1) and deeper depth (H_2), the coordinate of each block was obtained by summing the values of the bounding latitude and longitude and averaging it. This was used in plotting the midpoint of the coordinates. The main sources that account for the first layer average depth are the magnetic basement rocks. An estimated depth of 0.78 km to 1.25 km could be estimated from the first layer depth.

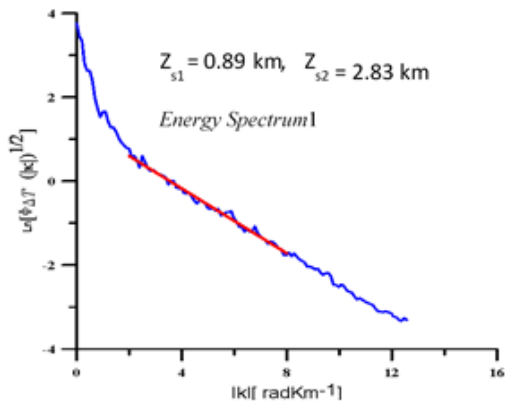


Figure 6a. Block1

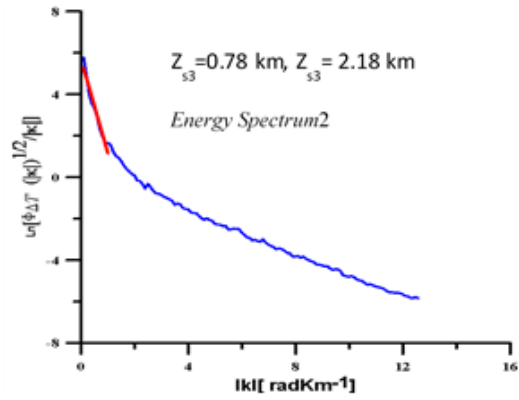


Figure 6b. Block1

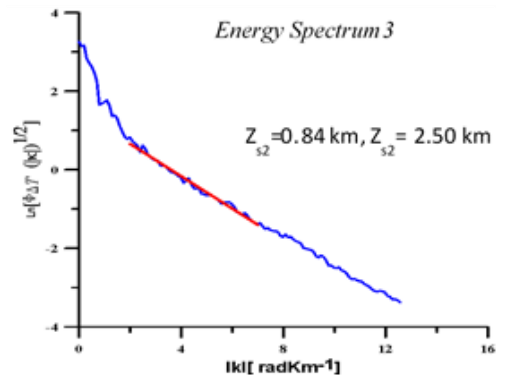


Figure 6c. Block2 Z_s

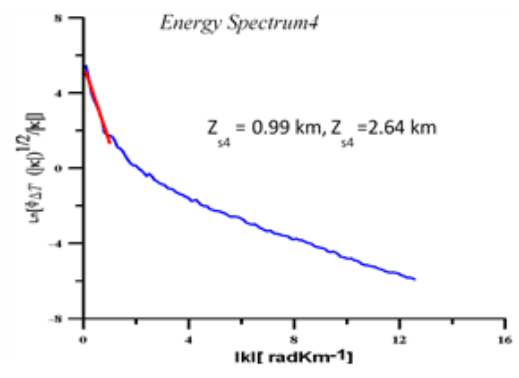


Figure 6d. Block1 Z_s

Figure 6 (a-d): Plots of energy spectrum against frequency for Section A to I

Table 2: Estimated depth to the shallow (depth1) magnetic sources and deep (depth2) magnetic sources in kilometers.

S/N	Spectral Blocks	Latitudes (X°)	Longitudes (Y°)	H ₁ (Km)	H ₂ (Km)
1	Block A	11.75	4.25	0.89	2.83
2	Block B	11.75	4.75	0.84	2.50
3	Block C	12.25	4.25	0.78	2.18
4	Block D	12.25	4.75	0.99	2.64
5	Block E	11.75	4.50	1.13	2.82
6	Block F	12.25	4.50	1.25	2.63
7	Block G	12.00	4.75	1.15	1.99
8	Block H	12.00	4.75	1.09	2.43
9	Block I	12.00	4.50	0.89	2.68

The second layer depth could be attributed to appreciable contrast in magnetization in the deeper parts of the basement rocks often caused by metamorphism due to intense heat. This depth

The highest depth of 2.83 km could be observed at the NS and SE part longitude 4.6°

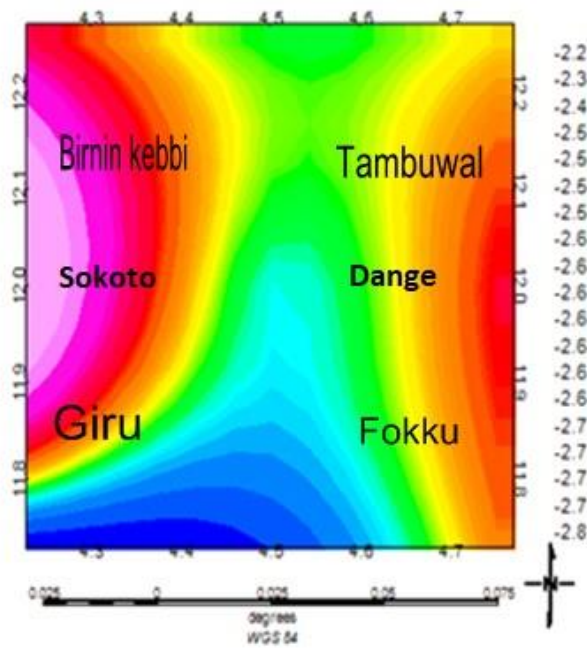


Figure 7: Contour map of second layer magnetic source depth (SPI) of the study area

4.6 Qualitative interpretation of source parameter imaging (SPI) map

The source parameter imaging (SPI) was applied to the TMI data over the study area. Figure 8 is the depth estimate obtained from the source parameter imaging. The white portions at the S - E and N - W part of the (SPI) map are the areas where the derivative used to estimate the local wavenumber are so small that the SPI structural index cannot be estimated reliably. The model-independent local wavenumber had been set to zero in that portion (Liu *et al.*, 1996). The (SPI) map shows

E and latitude 11.8° N SW of Guru town. The mid portion of the study area between Birnin-Kebbi Tumbuwal at the central part shows relatively higher depth of 2.60 km. The lowest depth of 1.99 km is located at E-W of Fokku, and at the NW part around Birnin Kebbi. Figures 7 (a - b) show the second layer depth of the study area. Careful observation of Figure 7 b shows that the area is depressed at the SW.

that the optimal sedimentary thickness or maximum depth to magnetic source rocks within the study area varies between 1738 m to 2308 m (1.73 km to 2.30 km). The highest depth can be found mostly at the SW part around Giru town. However, relatively higher depth scattered at the central, NW and SE part of the map.

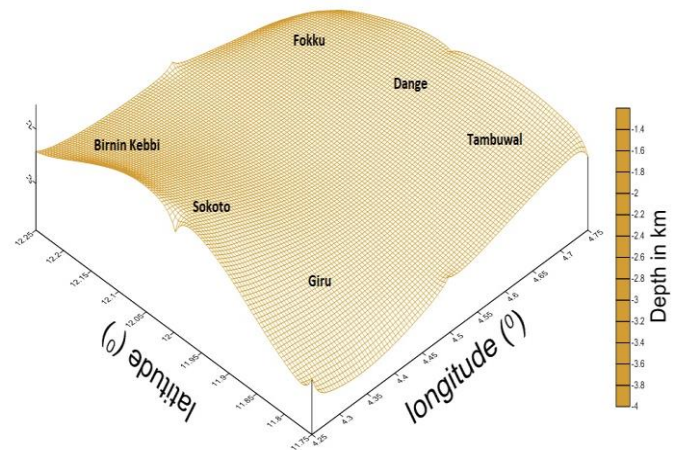


Figure 8: 3D-surface map of deeper magnetic source depth (SPI) of the study area

4.7. Sedimentary thickness and depth to magnetic source rocks within the study area

The depth to the underlying magnetic basement obtained from spectral analysis ranges from 1.99 km to 2.83 km as shown in Table 2. The source parameter imaging (SPI) result shows that the deeper part of the basin varies from 1.73 km to 2.30 km. The results

appeared to be in close agreement with one another, as the highest and the lowest depth obtained from spectral analysis slightly differs from that of source parameter imaging (SPI) analysis. The results obtained from both the spectral analysis of aeromagnetic data and source parameter imaging (SPI) are very much in agreement when compared with the works of other researchers within the basin. Kamba *et al.*, (2017) reported a maximum depth of 1.96 km at the lower Sokoto Basin Nigeria using spectral analysis, also Ofoha and Udensi (2014), later found basement depths within the range of 1.25 km to 1.80 km at the neighboring eastern part of the study area using spectral analysis method. The result also agrees with the findings of Kamba *et al.* (2017), who reported a maximum depth of 2.85 km for the entire Sokoto basin based on both spectral analysis and $2\frac{1}{2}$ D modeling of magnetic anomalies. Suleiman (2012) also reported a sediment thickness up to 1.72 km across Kebbi State within the basin using spectral analysis. Other researchers within the basin whose works agrees well with the results are; Ofoha and Udensi (2014), they reported a shallow depth up to 1.54 km across the Sokoto basin Nigeria using spectral analysis. Chikwelu and Ogbuagu (2014) obtained a deeper depth within the range of 0.6 km to 1.83 km in upper Sokoto basin using spectral analysis. However, Ofoha *et al.*, (2016) determine the magnetic basement depth in the northeastern part of Sokoto basin, using Source Parameter Imaging (SPI) and obtain a maximum thickness of 3.38 km.

5. CONCLUSION

Source parameter imaging (SPI) method was equally applied to evaluate the thickness of sediments or depth to magnetic source within the same area, and a maximum depth of 2.30 km were obtained at the southwestern part around Giru town while the lowest depth value of 1.73 km was obtained at the southeastern part around Fokku town. Upward continuation of the total magnetic intensity (TMI) values to various heights at 2 km, 5 km, 10 km, 15 km, 20 km and 25 km showed predominant tectonic trends in the E-W, NE-SW and NW-SE directions. The discontinuities correspond to

fracture zones that provide a channel for mineralizing fluids to get to the overlying sediments. The result obtained from the spectral depth analysis of the nine sections from the square block shows that the maximum depth of magnetic source rocks is found at Giru (2.83 km) and areas between Tambuwal and Birnin-Kebbi (2.60 km) respectively. Source parameter imaging was equally employed to estimate the thickness of sediments within the same area, and a maximum depth of 2.30 km was obtained around Giru. These are areas with relatively higher sedimentation, and are probable potential sites for hydrocarbon deposits.

6. RECOMMENDATIONS

In view of this research, it is recommended that profile modeling with integrated gravity analysis of the Sokoto Basin should be carried out to further study the basement depth and crustal thinning. Seismic reflection survey should also be carried out at Giru, Tambuwal as well as Birnin-Kebbi areas to determine and juxtaposed the stratigraphic sequence thickness within some prolific zones.

Since this work is based on aeromagnetic survey, I recommend that the ground gravity survey interpretation of this study area to be carried out in other to confirm the obtained result in this work.

REFERENCES

- Donovan, T. J., Forgery, R. L. and Robberts, A.A. (1979). Aeromagnetic detection of diagenetic magnetite over oil fields, *AAPG Bull.* **63**: 245 – 248.
- Geosoft Oasis Montaj, (2008). The core software platform for working with large volume gravity and magnetic spatial data; Geosoft Inc, Toronto, Canada.
- Hesham, S.Z., and Oweis, H.T. (2016). Application of High – pass filtering Techniques on Gravity and Magnetic Data of the Eastern
- Qattara Depression Area, Western, Desert, Egypt. *NRIAG. Journal of Astronomy and Geophysics*, 5(1); 106 – 123.
- Hinze, W.J. Von Frese, R.R.B. Saad, A.H. (2013). Gravity and Magnetic Exploration Principles, Practices, and Applications, Cambridge University Press, New York.
- Kogbe, C. A., (1979). Geology of southeastern portion of the

- Illummeden Basin (Sokoto Basin), *Bull. Dept. Geology, Ahmadu Bello University, Zaria, Nigeria*, 2, 420p
- Kogbe, C. A., (1981). Cretaceous and Tertiary of the Illummeden Basin Nigeria (West Africa), *Cretaceous Research* 2, 129 – 186.
- Kamba, A. H., and Ahmed, S. K., (2017). Depth to Basement Determination Using Sources Parameter Imaging (SPI) of Aeromagnetic Data, an Application to Lower Sokoto Basin, Northwest, Nigeria. *World Scientific News*, 40: 266-277.
- Langel, R. A., (1992). International Geomagnetic Reference Field: *Geophysics* 57, 956-959.
- Lasky, R.P., Mory, A.J. and Shevchenko, S. (1997). Structural Interpretation of Sedimentary Basin Using High – resolution Magnetic and Gravity data. *Exploration Geophysics*, 28(1), 247 – 251,
- Luyendyk, A. P. J., (1997). Processing of airborne magnetic data, *AGSO J. Australian Geol. Geophys.* 17, 31-38.
- Lala, T., Chaudhary, A. K., Patil, S. K., and Paul, D. K., (2011). Mafic dykes of Rewa Basin, central India: Implications on magma dispersal and petrogenesis; In: *Dyke Swarms* (ed.) Srivastava R K, Springer- Verlag, Berlin, pp. 141– 162.
- Lala, T., Mombasawala, L. S., Pande, K., and Paul, D. K., (2014). New ³⁹Ar–⁴⁰Ar ages of dykes from Madhya Pradesh and Chhattisgarh: Evidence for polyphase dyke intrusion in eastern Deccan Volcanic Province; *Curr. Sci.* 107, 1027– 1032.
- Lamontagne, M., Keating, P., and Perreault, S., (2003). Seismotectonic characteristics of the lower St. Lawrence seismic zone, Quebec: Insights from geology, magnetic, gravity and seismic; *Canadian J. Earth Sci.* 40, 317–336.
- Leech, D. P., Treloar, P. J., Lucas, N. S., and Grocott, J. (2003). Landsat TM analysis of fracture patterns: A case study from the Coastal Cordillera of northern Chile; *Int. J. Rem. Sens.* 24 3709–3726.
- Liu, G. D., Hao, T. Y., and Liu, Y. K., (1996). The significance of gravity and magnetic research for knowing sedimentary basin; *Prog. Geophys.* 11, 1–15 (in Chinese).
- McIntyre, J. I., (1980). Geologic significance of magnetic patterns related to magnetite in sediments and metasediments: a review, *Bull. Aust. Soc. Expl. Geoph* 11, 19-33.
- Miller, H.G., Singh, V., (1994). Potential field tilt—a new concept for location of potential field sources. *J. Appl. Geophys.* 32, 213–217.
- Minty, B. R. S., Milligan, P. R., Luyendyk, A. P. J., and Mackey, T. (2003). Merging airborne magnetic surveys into continental-scale compilations, *Geophysics* 68, 988-995.
- Obaje, N. G. (2009). Geology and mineral resources of Nigeria: Lecture Notes in Earth Sciences, Springer, Berlin Heidelberg.
- Obaje, N. G., Aduku, M. and Yusuf, I. (2013). The Sokoto Basin of northwestern Nigeria: a preliminary assessment of hydrocarbon prospectivity, *Petroleum Technology Development Journal* 3 (2), 66-80.
- Ofoha, C. C., Emujakporue G., Ngwueke, M. I., and Kiani, I., (2016). Determination of Magnetic Basement Depth over parts of Sokoto Basin, within Northern Nigeria, using Improved Source Parameter Image (ISPI) Technique. *Scientific News* 50, 266-277.
- Thompson, D.T., (1982). EULDPH: A new technique for making computer-assisted depth estimates from magnetic data. *Geophysics* 47 (1), 31–37.
- Verdusco, B., Fairhead, J.D., Green, C.M., Mackenzie, C., 2004. New insights into magnetic derivatives for structural mapping. *Lead. Edge* 23, 116–119.